SINTEF

Predicting near-time satellite signal attenuation at Ka-band using tropospheric weather forecast model

Knut Grythe, Lars Erling Bråten, Snorre Stavik Rønning, Terje Tjelta

Predicting near-time satellite signal attenuation at Ka-band using tropospheric weather forecast model

Knut Grythe[1], Lars Erling Bråten[2], Snorre Stavik Rønning[3], Terje Tjelta[4]

[1] SINTEF, Trondheim, Norway, knut.grythe@sintef.no

[2] Norwegian Defence Research Establishment, FFI, Kjeller, Norway, lars-erling.braten@ffi.no

[3] Norwegian Meteorological Institute, Oslo, Norway, snorresr@met.no

[4] University of Oslo, Norway, terje.tjelta@its.uio.no

Abstract—There are satellite communication applications where it is desirable to predict near time (e.g. 2 to 12 h) propagation losses at Ka-band due to hydrometeor precipitation. We present results from a project investigating the possibility and quality of short term prediction of satellite link attenuation at Ka-band. The starting point is a 67 h near time numerical weather prediction data from the Norwegian Meteorological Institute. A period of 3 months and for 3 sites in Norway have been studied. Based upon these accumulated 9 months of data, the precipitation along the satellite link to the ground terminal is calculated for every hour. The attenuation results from the model is compared to high accuracy contemporary measurements of the same path. If the forecast is predicting the presence of precipitation correctly, the predicted attenuation error has a low bias and the standard deviation value is typically in the order of 1.5 dB.

Keywords—Attenuation prediction; weather forecast; satellite links; Ka-band;

I. INTRODUCTION

The influence of the atmosphere on radio signals between Earth and space depends upon the carrier frequency. The carrier frequency bands are generally split in a band below 3 GHz and a band above 3 GHz [1] where the crossover is not a fixed value, but subject to site positions, signal properties and time of year. Signals in the lower band are influenced by processes in the ionosphere due to e.g. solar activities while signals in the upper band are mainly affected by processes in the troposphere like the amount of precipitation.

The availability of a satellite link meeting a guaranteed quality in terms of bit error rate (BER) or availability for a given amount of time is important for the users of the satellite communication services. Traditionally there are two mechanisms applied for dimensioning or adapting the availability of a satellite link operating at higher frequencies like Ku - and Ka bands. First, for long-term availability statistics e.g. an ITU rain map [2] can be used to find the rain intensity in a region for a given percentage of time, like 99.99% availability. These results are used as contributions when setting link margins in the design of satellite systems. Secondly, short time link quality adaptations within seconds or minutes, are obtained via

e.g. the application of adaptive coding and modulation (ACM) like in the DVB-S2 standard.

Situation awareness is a general term used for the perception of important environmental elements and events with respect to time and space used in both military and critical civilian operations. Awareness is obtained among others via satellite navigation - and communication systems. The quality of awareness is determined by the quality and availability of the supporting satellite systems. The focus of this paper is on propagation situation awareness obtained via precipitation forecast in the troposphere obtain from numerical weather prediction (NWP) models. The forecast time window is in the order of 2 to 12 hours or more, depending upon the time lag of the forecast model. From the above we can observe that this concerns high frequency signals, typically most affected above 10 GHz where the attenuation is highest.

Targeting improved deep space communication at Ka-band, [7] presents work on comparing the prediction of variation in atmospheric noise temperature and attenuation obtained via weather modelling and water vapor radiometer. They found that 2 dB increase in data return was possible using weather prediction.

The contribution of this paper is to utilize the availability of high quality measurements of Ka-band pilot signal attenuation [8] as quality validation to obtain error statistics for attenuation predictions obtained via NWP for the same signal path as the pilot. The probability of the NWP to correctly predict rain present, is also evaluated.

The paper is organized as follows. Motivations and potential user groups of the forecast are initially presented as a background for the following sections. Weather modeling and prediction approach are given in Section III with some results indicating the forecasting quality in Section IV. A conclusion is given in Section V.

II. Background and motivation

A. Background

Estimating precipitation along a signal path based upon precipitation measurements at the ground terminal site is only generally viable when a satellite is at high elevation angles. As the elevation angle decreases; distant parts of the path can be affected by precipitation not observed at a terminal site as illustrated in Fig. 1.

Predicting rain events at distant space and time is only possible via input from meteorological forecast models. Radars can be used, but the forecast will only be reliable just for a short time ahead.

B. Application groups

Weather forecasts present an overall prediction of the expected precipitation in the near future, (for our study 1 h to 67 h in 1 h steps) based upon advanced weather models. This opens the opportunity for predicting the signal attenuation due to precipitation some hours ahead, based upon the use of weather forecasts. Knowing the position of both the user ground terminal and the satellite, the signal path through the troposphere can be calculated and the rain intensities along the path predicted. An estimate of the signal attenuation can be derived from this information.

The user groups that will benefit from a service based upon propagation predictions include:

- Users who want to download/transmit large amount of data with optimum real time requirements.
- An operator can predict the available capacity in various geographical areas and thus plan the capacity distribution in time and space for the coming hours.
- An operator can use this for diversity planning or planning of equipment maintenance.
- An owner or operator of a remote sensor network can plan the time of data transfer to a more beneficial attenuation period and thereby save transmitter energy. This saves money as the maintenance interval for the energy sources can increase.
- Help planning of switching between hubs for high elliptical orbit (HEO) satellites.
- Planning and controlling the operation of drones where the autonomy and robustness requires access to satellite communication.

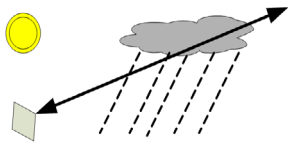Generally, routine problems with the communication links are often difficult to distinguish as to origin – are they manmade or natural? Degradation to critical services may be masked by e.g. tropospheric disturbances. Being able to predict tropospheric degradation will help reveal manmade interference - and disturbance events. This contributes to raise the confidence in the communication solution.

III. PREDICTION CONCEPT

We utilised a grid of model data surrounding the signal path investigated, to enable characterisation of rain events. The altitude dependent data are represented within 11 constant pressure grid surfaces, and improve the understanding of when rain occurs with forecasts in 3-dimentions in addition to time. The predicted incremental attenuation along the path is calculated via the procedure of [9] given the predicted rain at a path point and then summed to get the total path attenuation due to precipitation.

A. Meteorological model

The model data is delivered from the Norwegian Meteorological Institute (NMI) in a Network Common Data Form (NetCDF) format [3]. This format is readily read by Matlab, the computational software selected for this project. The model data is taken from the AROME-MetCoOp model [4]. There is 2.5 km horizontal distance between points in each grid surface. A new model structure is generated every 6 h and each model structure contains hourly predictions from 1 to 67 h ahead of the model run. The main results are given in the model surfaces, where only a subset is stored. However, interpolated values are stored for 11 pressure surfaces.

To calculate the height of a grid point in the model based on its pressure level, we can use the geopotential value of that point. The geometrical height above sea level (Z) for a point is given by [5]

$$Z = \frac{RH}{\frac{g_l R}{9.80665} - H} \quad (1)$$

where

- $Z =$ geometric height above mean sea level in meters
- $R =$ radius of earth at a given latitude, in meters
- $H =$ geopotential altitude in geopotential meters
- $g_l =$ actual acceleration of gravity at mean sea level at the given latitude l

H is calculated by using the definition of the geopotential meter (gpm) [6]

$$gpm = 9.80665 \frac{m^2}{s^2} \quad (2)$$

By using the equation above and the geopotential Φ from the model, we get

$$H = \frac{\Phi}{9.80665} gpm \quad (3)$$

Fig. 1 Illustration of distant rain in the signal path for low elevation.

The earth radius is [5]

$$R = \frac{2g_l}{-\left(\dfrac{\delta g}{\delta Z}\right)_{Z=0}} \quad (4)$$

where

$$-\left(\frac{\delta g}{\delta Z}\right)_{Z=0} = \begin{matrix} 3.085462*10^{-6} + 2.27*10^{-9}\cos(2l) - \\ -2*10^{-12}\cos(4l) \end{matrix} \quad (5)$$

The actual gravity at a specific latitude is represented by the "WGS 1984 Ellipsoidal Gravity Formula"

$$g_l = 9.7803253359\left[\frac{1+0.00193185265241\sin^2(l)}{\sqrt{1-0.00669437999013\sin^2(l)}}\right]ms^{-2}$$

Thus we have 11 realizations of each variable corresponding to latitude, longitude and time variant height pattern.

An example of a plot of air temperature at 1000 hPa as a function of latitude and longitude is shown in Fig. 2. The 3-d model data have enough information to make a good estimate of the hydrometeor precipitation rate in each model point, but a terminal drop velocity had to be fixed. In the analyses shown in this paper 5 m/s was used. The ground 2-d data provided the accumulated precipitation amount in mm.

B. Precipitation interpolation

The attenuation rates describes later are based on interpolated values of the meteorological data along the path between the terminal and the satellite. The path was divided into segments of 1 km length. For each end point of the segments, rain intensity was estimated based on interpolation of the values in the 11 pressure surfaces.

The nearest 4 data locations below the point of interest and the 4 above were first identified. The points below were selected within the same pressure surface, and the points above within the higher surface. The 3 nearest geographical locations were found and then barycentric interpolation performed to find the location value in each layer. The linear interpolation was applied to get the final value in between the layers.
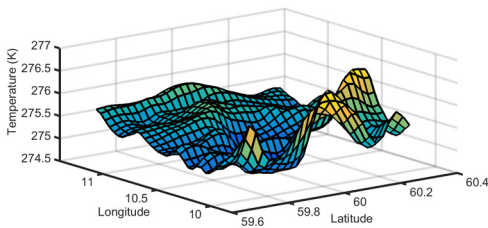

Fig. 2 Example of air temperature at 1000 hPa variations as function of latitude and longitude

IV. VALIDATION PRREDICTION RESULTS

The results of the predictions are validated against high quality Ka-band measurements at 19.68 GHz for a period of three months, June to August, 2015 at integer hours [8]. The sites are Eggemoen, Nittedal and Kjeller in Norway resulting in overall nine months of data. The Ka-measurements for the first two locations are carried out under a project for the European Space Agency (ESA), obtaining long-term beacon level data with a sampling rate of 10 Hz. The satellite is Eutelsat Ka-Sat at 9 degrees East.

A. Type of analyses

The analyses are presented in terms of two types of reference data.

- Rain present/not present

One classification of the Ka-band measurements is in terms of rain present/not present. This classification is suitable for evaluation of the capability of the predictor to hit the correct time instances when rain is present/not present.

- Comparison of the attenuation values measured at Ka-band and those found via weather model predictions.

This indicates the capability of the predictor to correctly calculate the attenuation value given that both methods indicate rain present. Here the Ka-measurements are given one hour mean value; that is as the average over +/- 30 minutes from the integer valued hours since the weather model is giving forecasts for integer hours.

From these two approaches, we can deduce the following statistics:

- Probability of predicting the rain correctly: P_{Hit}

This is the probability that the rain is predicted to be present, given that the Ka-measurements indicate rain.

- Probability that the predictor is missing the rain: P_{Miss}

This is the probability that the rain is predicted to be absent, given that the Ka-measurements indicate rain.

- Probability of false rain alarm P_{False}

This is the probability of predicted rain when the Ka-measurements indicate no rain. *A good predictor for our purposes should have a high P_{Hit} and a lowest possible P_{False}.*

- The predictor attenuation error probability $p_{KaPd}(\varepsilon)$

The prediction error is defined as $\varepsilon = KaAtt - ModAtt$ in dB;
That is the difference between the Ka measured attenuation and the predicted attenuation.

- CDF, standard deviation and mean values for the predicted attenuation errors.

We present some results from Nittedal and Eggemoen sites in the following sub sections, illustrating typical prediction behaviours valid for all three sites and all prediction legs.

The analysed legs were 3, 6, 9 and 12 hours ahead and all were analysed over a window of 6 hours. The prediction legs are defined as follows. E.g. leg 3 corresponds to predicted attenuations over a period of 6 hours for the time instants

$t_0 + 3:8$ hours, where t_0 is the model release time. $t_0 = \{00, 06, 12, 18\}$, that is 4 times every 24 h. Leg 9 corresponds to predicted attenuations over a period of 6 h for the time instants $t_0 + 9:14$ h.

B. Site Nittedal (60°4'23"N 10°52'20"E)

Two types of figures are shown. The first represents the CDF of the measured attenuation at Ka-band and the predictions. The predictions encompass application of both model layers and the accumulated amount of rain on the ground over a period of one hour, denoted as "Layer" and "Ground". Fig. 1 is the first example of the CDF.

The second type of figures contain the prediction error CDF, including first and second order statistics moments. In addition, the probabilities of hit and false rain alarm values are shown. Fig. 2 is the first example of this. The three months are June, July and August 2015 as can be observed from the x-axis of Fig. 4. The top sub plot of Fig.4 shows the error in the predictions for layer and ground rain. The two different legs are 3 in Fig. 4 and 9 in Fig. 5.
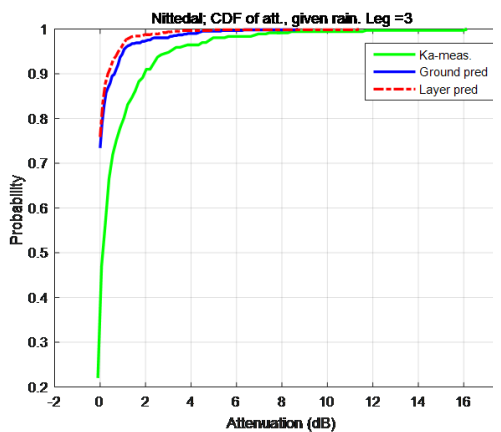

Fig. 5. Prediction errors and corresponding CDF, given that measured rain is true.

C. Eggemoen (60°12'58"N 10°19'17"Ø)

The second site is Eggemoen that is west of the Nittedal site where the same statistical results are given. The prediction and measurements CDF in Fig. 5 for leg 3, and the error statistics in Figs. 6 and7 for leg 3 and leg 9, respectively.

Fig. 3. CDF of the predicted and measured attenuation, given rain. Leg = 3.
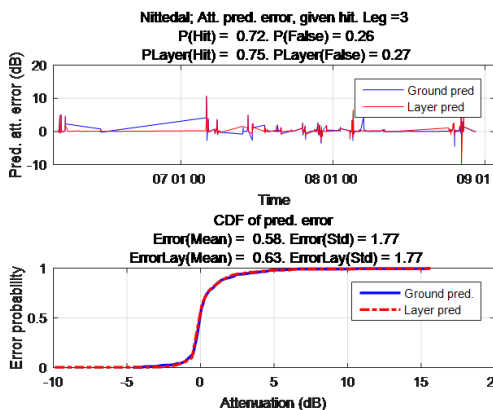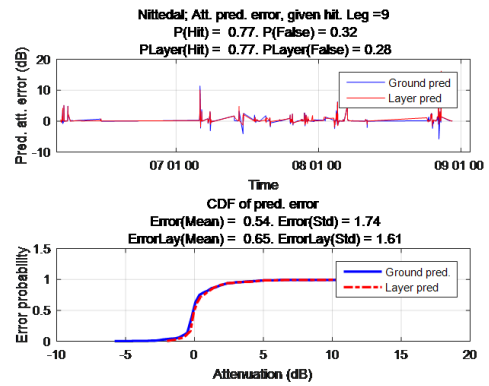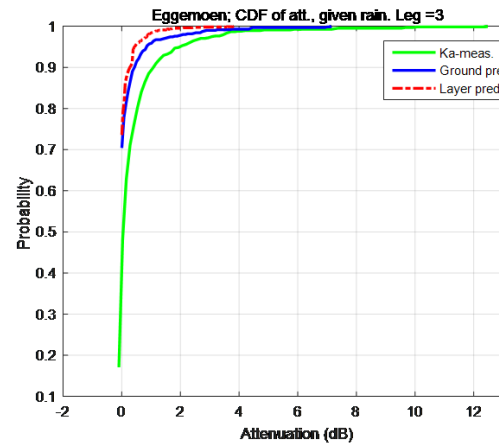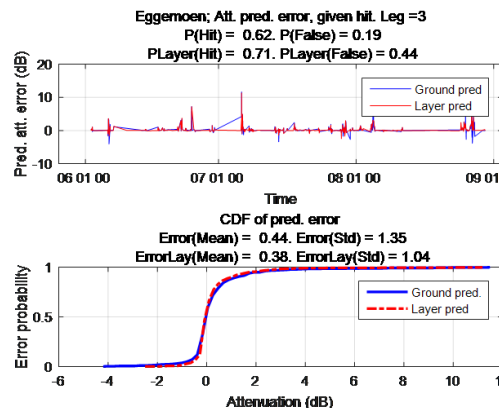

Fig. 6. CDF of the predicted and measured attenuation.

Fig. 4. Prediction errors and corresponding CDF, given that measured rain is true.

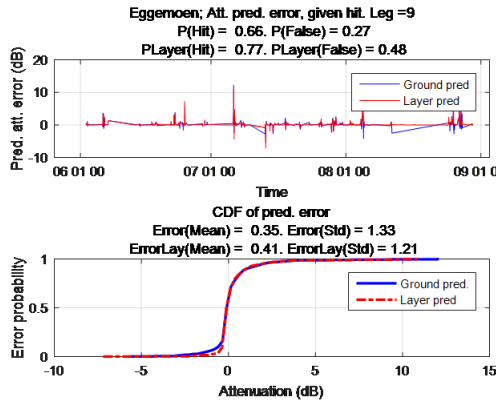Fig. 7. Prediction errors and corresponding CDF, given that

Fig. 8. Prediction errors and corresponding CDF, given that measured rain is true

D. Prediction model results

The following two tables summarise the statistical parameters depicted in the previous figures.

	Nittedal			Eggemoen		
Leg (H)	P(Hit)	P(False)	Error(dB) Mean/Std	P(Hit)	P(Fa)	Error(dB) Mean/Std
3	0.72	0.26	0.57/1.8	0.62	0.2	0.44/1.4
6	0.74	0.3	0.55/1.8	0.66	0.23	0.4/1.3
9	0.77	0.32	0.54/1.7	0.66	0.27	0.35/1.3
12	0.77	0.33	0.57/1.8	0.68	0.29	0.35/1.3

Table 1. Ground layer; Values of some relevant statistical parameters

	Nittedal			Eggemoen		
Leg (H)	PL (Hit)	PL (False)	Error(dB) Mean/Std	PL (Hit)	PL (Fa)	Error(dB) Mean/Std
3	0.75	0.27	0.63/1.8	0.71	0.44	0.38/1.0
6	0.76	0.27	0.63/1.7	0.78	0.50	0.4/1.0
9	0.77	0.28	0.65/1.6	0.77	0.48	0.4/1.2
12	0.77	0.27	0.7/1.7	0.67	0.42	0.36/1.1

Table 2. All layers; Values of some relevant statistical parameters

The results indicate that the hit probability is mostly larger than 65 to 70%. At the same time, the false alarm rate is mostly below 25%, although Eggemoen is just below 50%. From the attenuation CDFs, we can see that both prediction methods predict attenuations that are typically lower that what is measured. From the two tables and the previous figures, it appears that the hit probability is varying from site to site and with somewhat different results for the ground and layered approach. The same goes for the false alarm rate. Besides from possible weaknesses in the tested attenuation prediction methods, the weather model outputs may also have a varying correctness from site to site and consequently influencing the site dependent prediction quality. The results are generally encouraging and support the hypothesis that prediction based upon weather models is applicable for propagation forecasting.

V. SUMMARY

The precipitation hit-rate of the meteorological forecast model AROME at the tested sites over an accumulated period of 9 months is better than in the order of 65 to 70 percent, with a clear site dependency. Given precipitation hit, we found that the prediction of the signal attenuation has an error with a typical bias and standard deviation in the order of 0.5 to 0.5 dB and 1.0 to 1.7 dB respectively for prediction legs from 3 to 12 hours. These are encouraging results supporting the hypothesis that the user groups introduced in section 2 could benefit from a service based such predictions.

ACKNOWLEDGMENT

REFERENCES

[1] Louis. J. Ippolito Jr. "Satellite communication systemes engineerin - Atmospheric effects, satellite link design and system performance". John Wiley & Sons Ltd. 2008.

[2] Characteristics of Precipitation for Propagation Modelling, ITU-R Recommendation P.837-6, 2017, Int. Telecommun. Union, Geneva.

[3] Network Common Data Form (NetCDF), http://www.unidata.ucar.edu/software/netcdf/, page visited 2015.11.21

[4] Meteorological Co-operation on Operational NWP (Numerical Weather Prediction), AROME-MetCoOp, Norwegian Meteorological Institute and Swedish Meteorological and Hydrological Institute, web page http://metcoop.org/memo/.

[5] Robert J. List," Smithsonian meteorological tables," 6th ed., 1951.R. Nicole, "Title of paper with only first word capitalized," J. Name Stand. Abbrev., in press.

[6] "U.S. standard atmosphere", National Oceanic and Atmospheric Administration, 1976.

[7] David Morabito, Longtao Wu and Stephen Slobin "Weather forecasting for Ka-band operations". IPN Progress report 42-206 – August 15,2016.

[8] Tjelta, Terje; Rytír, Martin; Bråten, Lars Erling; Grotthing, Per Arne; Cheffena, Michael & Håkegård, Jan Erik (2017). Results of a Ka Band Campaign for the Characterisation of Propagation Conditions for SatCom Systems at High Latitudes, In *2017 11th European Conference on Antennas and Propagation (EUCAP), 19-24 March 2017*.

[9] Specific attenuation model for rain for use in prediction methods. Rec. ITU-R P.838-3, 2005.